International Immunopharmacology 75 (2019) 105795

Contents lists available at ScienceDirect

International Immunopharmacology

journal homepage: www.elsevier.com/locate/intimp

Potential role of M2 macrophage polarization in ventilator-induced lung fibrosis

Lu Wang[a,b], Yi Zhang[a,b], Nannan Zhang[a,b], Jingen Xia[a,b], Qingyuan Zhan[a,b,*], Chen Wang[a,b,c,**]

[a] Department of Pulmonary and Critical Care Medicine, China-Japan Friendship Hospital, China
[b] Center for Respiratory Diseases, National Clinical Research Center for Respiratory Diseases, China
[c] Chinese Academy of Medical Science, Peking Union Medical College, China

ARTICLE INFO

Keywords:
Ventilator-induced lung injury
Pulmonary fibrosis
Macrophage polarization
Epithelial–mesenchymal transition

ABSTRACT

Mechanical ventilation (MV) is an essential life-support technique, but it can induce ventilator-induced lung injury (VILI) and subsequent pulmonary fibrosis. The mechanisms underlying this fibrosis are largely unknown. Because excessive polarization of M2 macrophages has increasingly been cited as possible inciting factor for tissue remodeling and organ fibrosis, we here hypothesize it might be involved in the development of pulmonary fibrosis after high tidal volume (VT) MV. In our prospective, randomized, controlled animal study, C57BL/6 mice were randomly placed in either a VILI group or sham group. After ventilation, surviving mice were allowed to recover for 0, 1, 3, 5, 7, or 14 days. 200 mice were involved in our in vivo experiment, and the results calculated here refer only to the surviving mice. The results clearly showed that high-VT MV caused early inflammation and a subsequent fibroproliferative response in mice without pre-existing lung disease. High-VT MV was also found to lead to a dramatic increase in the number of M2 macrophages in mouse bronchoalveolar lavage fluid (BALF) cell and lung tissues. Consistent with the progression of fibrosis, there were far more M2 macrophages at the 5th day after ventilation and remained dominant for 2 weeks. High-VT MV induced epithelial–mesenchymal transition (EMT) on day 7, accompanied by the increased expression of TGF-β1 and p-Smad2/3. In vitro experiments, the co-culture of M2 macrophage and MLE-12 cells resulted in a significant EMT and upregulation of TGF-β1 and p-Smad2/3 in MLE-12 cells. To summarize, our findings suggested the persistent tilt polarization toward M2 macrophages was associated with EMT during the course of ventilator-induced pulmonary fibrosis, which may play its roles through activation of epithelial TGF-β1/Smad2/3 signaling.

1. Introduction

Over the past few decades, mechanical ventilation (MV) has become one of the most important life support techniques [1]. However, numerous studies have demonstrated that MV with inadequate ventilator settings can cause secondary injury that exacerbates lung injury and mortality toward critically ill patients. It is called ventilator-induced lung injury (VILI) and pathologically characterized as inflammatory-cell infiltration, hyaline membranes, vascular permeability, and pulmonary edema [2,3]. The emergence of VILI not only affects the clinical efficacy, but also acts as an important contributor to pulmonary fibrosis [4,5].

Currently, volutrauma, atelectrauma, and barotrauma are recognized as the major mechanisms underlying VILI [2,3], but the mechanisms underlying the pulmonary fibrosis that follows VILI still remain to be characterized. Per available data, it can be described as a more subtle form of biological injury that involves neutrophils, alveolar epithelial cells, immune-cells and their cytokines, adhesion molecules, and mediators, which set the stage for the progression of pulmonary fibrosis [2].

Pulmonary macrophages are the most numerous immune cells present in the lung and alveolar space [6,7]. Many studies have shown macrophages are sufficiently plastic to adopt different activation states within specific signals. The key components of their biological response, including recruitment, differentiation, polarization, function, and cellular interactions, are largely dependent on the presence and severity of local inflammation [6]. Recently, M1 and M2 are the most commonly recognized phenotypes of macrophages, although the use of terms M1 and M2 remains controversial because of the lack of tightly defined criteria for scoring phenotypes [8]. Specifically, M1, also

* Correspondence to: Q. Zhan, No 2, East Yinghua Road, Chaoyang District, Beijing 100029, China.
** Correspondence to: C. Wang, No 9, Dong Dan San Tiao, Dongcheng District, Beijing 100005, China.
E-mail addresses: zhanqy0915@163.com (Q. Zhan), wangchen66366@163.com (C. Wang).

https://doi.org/10.1016/j.intimp.2019.105795
Received 8 February 2019; Received in revised form 30 July 2019; Accepted 30 July 2019
Available online 14 August 2019

known as classically activated macrophages (CAMs), are induced by toll-like receptor (TLR) and interferon signaling and are related to the production of proinflammatory factors such as inducible nitric oxide synthase (iNOS), interleukin-1β (IL-1β), tumor necrosis factor-alpha (TNF-α). M2, also called alternatively activated macrophage (AAMs), can be stimulated with interleukin-4 (IL-4) or interleukin-13 (IL-13), and hallmarked by production of interleukin-10 (IL-10), arginase 1 (Arg-1), found in inflammatory zone 1 (FIZZ1), transforming growth factor-β1 (TGF-β1), and platelet-derived growth factor (PDGF) [6]. The process by which macrophages have been activated at an indicated point in space and time is here referred to as macrophage polarization [8].

Data show that macrophage polarization is critical to the initiation and resolution of lung inflammation [6]. For example, polarization of M1 macrophages always occurs during the early stage of injury, and it is associated with proinflammatory response, clearing bacteria and tumoricidal activity, whereas M2 macrophages play important roles in coordinating inflammation abrogation, and immunosuppression. The self- limiting properties of macrophage polarization are essential to eliminating foreign materials. They aid in tissue repair and eventually return the tissue to homeostasis [8]. Some investigations have confirmed that they have a significant role in the excessive reprograming of M2 macrophages in driving the fibrotic response in lung disorders, such as idiopathic pulmonary fibrosis (IPF) and ARDS-associated fibrosis [6,9]. However, to our knowledge, the role of M2 macrophage polarization has never been explored in the context of ventilator-induced lung fibrosis in mice without pre-existing lung disease.

Prior to this study, we determined that the pulmonary fibrosis caused by 4 h of high-VT MV was most pronounced on the 7th day [10]. Through comparison of the sham and VILI mice on days 0 and 7, our previous RNA sequencing showed upregulated activations of epithelial recruitment, proliferation, migration and differentiation, suggesting a potential role of alveolar epithelial cells as important sources of inflammatory cascade link to VILI and pulmonary fibrosis [10]. Thus, in our present study, we aimed to explore the dynamic changes of lung macrophage polarization in the evolution of pulmonary fibrosis after VILI, and the possible mechanism involved between macrophages and alveolar epithelial cells, which may pave the way to innovative mechanisms and therapeutic approaches.

2. Materials and methods

2.1. Mouse model of VILI

Specific-pathogen-free, male C57BL/6 mice (Institute of Laboratory Animal Sciences, Beijing, China) were randomly divided to VILI group and sham-operated controls. All animals were anesthetized with an intraperitoneal injection of pentobarbitone (100 mg/kg, Pfizer, Ireland). After confirming depth of anesthesia by absence of response to paw compression, the neck skin of mice were cut, blunt dissection, expose the trachea; mice were then subjected to endotracheal intubation by using a 22G Teflon catheter and the trachea hold with catheter were ligated to prevent air leaks. Mice in model groups were then mechanically ventilated with a small animal ventilator ((55–7040, VentElite; Harvard Apparatus, Holliston, MA, US) for 4 h using VT of 20 mL/kg plus 0 cm H_2O positive end-expiratory pressure (PEEP) and fraction of inspiration O_2(FiO_2) 0.4, respiratory rate 80 breaths/min, inspiratory-expiratory ratio 1:1 [11,12]. During the ventilation period, mice were given pentobarbitone (50 mg/kg) as needed; the cocuronium besylate (0.6 mg/kg, H20130486; MSD Performance Products, Kenilworth, NJ, US) was intraperitonealy administered once per hour to achieve muscle relaxation. 4 h later, animals were sent back to the facilities, where they were given free access to water and food. Mice that were anesthetized, and intubated, but that continued spontaneous breathing (SB) served as the sham group. The study was approved and guided by the Animal Care Review Committee of Capital Medical University (No. AEEI-2016-168, Beijing, China).

2.2. Sample collection

Surviving animals were euthanized with cervical dislocation at 0, 1, 3, 5, 7 and 14 days, respectively. The tracheas were cannulated and the lungs were lavaged three times with 1 mL pre-cold phosphate-buffered saline (PBS). The cell-free bronchoalveolar lavage fluid (BALF) supernatants were used for total protein measurement, while the BALF cells were collected for flow cytometry. Lung wet-to-dry weight ratios were determined with unlavaged left lungs, and remaining tissues were respectively separated for the histological evaluation, immunostaining, flow cytometry and protein analysis.

2.3. Lung histopathology and immunohistochemistry

Lung sections were fixed with 10% neutral formalin for 1 week, and then dehydrated, embedded, and sliced at 5-μm thick intervals for hematoxylin and eosin (H&E) staining. The severity of microscopic lung injury [13] and fibrosis scores [14] were then graded. The Masson's trichrome and Picrosirius Red stain were used for collagen deposition area and type analysis. For immunohistochemistry, the sections were stained with antibodies against E-cadherin (1:100 diluted, ab76055, Abcam, UK), vimentin (1:50 diluted, 10366-1-AP, Proteintech, US), fibronectin (1:50 diluted, 15613-1-AP, Proteintech), α-SMA (1:100 diluted, A2547, Sigma-Aldrich, US). The mean density of the positive areas in sections was calculated using Image Pro-Plus 6.0 software (Media Cybernetics, US).

2.4. Immunofluorescence

OCT embedded lung slices were first blocked with 5% bovine serum albumin (BSA) and then soaked in 0.1% Triton X-100. Slices were then incubated with primary antibodies against F4/80 (1:200 diluted, ab6640, Abcam), Mac3 (1:200 diluted, ab18528) at 4 °C overnight, followed by incubation with secondary antibodies. Lastly, the stained sections were visualized on a fluorescent microscope (Olympus, Japan). Antibodies of iNOS (1:100 diluted, ab15323, Abcam), Arg-1 (1:200 diluted, ab91279, Abcam) were used for cell immunofluorescence.

2.5. Hydroxyproline assay

Lung hydroxyproline content was measured by using the hydroxyproline assay kit in accordance with manufacturer's instructions (A030-2, Nanjing Jiancheng, China). The data are here expressed as micrograms of hydroxyproline per gram of wet lung tissue.

2.6. Flow cytometry

BALF cells and fresh tissue homogenates were passed through a 100 μm cell strainer and resuspended in fluorescence-activated cell sorting (FACS) buffer (PBS plus 2 mM EDTA). They were then blocked with 5% BSA, and stained with corresponding antibodies for 30 min at 4 °C in the dark. The following antibodies were used: PerCP Rat Anti-CD45 (1:200 diluted, 557235, BD Biosciences, US); FITC Rat Anti-CD11b (1:200 diluted, 557396, BD Biosciences); PE Rat Anti-F4/80 (1:400 diluted, 565410, BD Biosciences) and Alexa Fluor647 Rat Anti-CD206 (1:200 diluted, 565250, BD Biosciences). Dead cells and debris were excluded by using forward scatter/side scatter (FSC/SSC), and analysis was performed using FlowJo VX software (Treestar, US).

2.7. Western blot

Fresh lung homogenates and cell lysates were quantified boiled, and resolved on 10% (Sodium dodecylsulphate polyacrylamide gel electrophoresis) SDS-PAGE gels. After electrotransfer onto polyvinylidene fluoride (PVDF) membranes, blots were blocked and incubated with primary antibodies against E-cadherin (1:1000 diluted), vimentin

(1:2000 diluted), fibronectin (1:2000 diluted), α-SMA (1:3000 diluted), TGF-β1 (1:500 diluted, ab92486, Abcam), p-smad2/3 (1:500 diluted, 8828, CST, US), smad2/3 (1:1000 diluted, 8685, CST), and GAPDH (1:5000 diluted, 60004-1-Ig, 60004-1-Ig, Proteintech), or β-tubulin (1:5000 diluted, 66240-1-Ig, Proteintech), β-actin (1:5000 diluted, 60008-1-Ig, Proteintech). The next day, the blots were incubated with horseradish peroxidase-conjugated secondary antibody and visualized by using chemiluminescent reagents (Millipore, US).

2.8. Isolation and identification of bone-marrow-derived macrophages

Bone-marrow-derived mononuclear cells were isolated from 10 to 12 week old male C57/BL/6 mice using Ficoll-Paque gradient centrifugation [15]. In brief, after the muscle was trimmed off, the bone marrow cells were flushed from the bone shafts with pre-cold PBS. Then cells were resuspended to break up any cell aggregates and subjected to Ficoll-Histopaque (1.083 g/mL) at 820 ×*g* for 20 min. The white cell layer at the interface was harvested and then washed twice with PBS at 220 g for 5 min. Then the cells were filtered through a 70 μm cell strainer and resuspended in Dulbecco's modified Eagle medium (DMEM, Lonza, Life Technologies) supplemented with 20% fetal bovine serum (FBS, Gibco, Australia), 100 units/mL penicillin, 100 μg/mL streptomycin and 2 mmol/L glutamine. According to a modified version of the method reported by Beckley K. Davis [16], mouse granulocyte-macrophage colony-stimulating factor (GM-CSF, 96-315-03, Peprotech, US) were used to induce mature macrophage (M0) for 8 days at the final concentration of 50 ng/mL. The nonadherent cells were discarded. The remaining adherent cells were cultured for further macrophages polarization. M1 macrophages were polarized by using LPS (055:B5, L6529, Sigma-Aldrich, US) and IFN-γ (315-05, Peprotech) at the respective concentrations of 100 ng/mL and 20 ng/mL, while M2 macrophages were differentiated with IL-4 (214-14, Peprotech) and IL-13 (210-13, Peprotech) at the dose of 20 ng/mL and 10 ng/mL, respectively. Finally, the polarized phenotype was evaluated using immunofluorescence or flow cytometry (BD FACS Fortessa, DB Biosciences, US) analysis with cell surface antigens CD45, CD11b, F4/80, and CD206 [17].

2.9. Coculture experiments

Mouse lung epithelial cell line (MLE-12, ATCC, US) and primary macrophages were co-cultured using Transwells (3422, Corning, MA, US) with a membrane pore size of 8 μm [18]. MLE-12 cells were seeded into upper 24-well plates at a density of 6×10^3 cells per wells, and primary M0, M1, and M2 macrophages were seeded into the lower chamber. PBS and TGF-β1 (10 ng/mL, 100-21, PeproTech) co-culture groups were served as the controls [19]. 48 h later, cell morphology, the expression levels of vimentin, fibronectin, α-SMA, and TGF-β1, smad2/3 and p-Smad2/3 were (Nikon Eclipse Ti, Japan) subsequently measured.

2.10. Statistical analysis

Data were analyzed by using one-way analysis of variance (ANOVA), and represented as mean ± SD using GraphPad Prism 7.0 (GraphPad, US). $P < 0.05$ was considered statistically significant.

3. Results

3.1. Inflammatory and fibroproliferative responses during resolution and repair after ventilation

As shown in Fig. 1A, mice with high-VT ventilation caused obvious alveolar damage, hemorrhage, and inflammatory cellular infiltration within 24 h. On days 3 through 5, it showed a decline in pulmonary inflammatory response, and slow repair in lung structure. By the 7th to 14th day, it developed into a significant lesion that mainly manifested as thickened alveolar septum and cell proliferation [10]. As shown under Masson (Fig. 1B) and Picrosirius Red staining (Fig. 1C), mice with high-TV MV resulted in significant lung damage and collagen deposition (mainly type I) in lung interstitium and around airway and vessels, which were most pronounced at 7th day (Fig. 1D–G). Additionally, the total protein of BALF and the wet-to-dry weight ratio were significantly raised in VILI group on day 1, while lung hydroxyproline contents were most described in VILI group on day 7 (Fig. 1H–J).

3.2. Dynamic changes in macrophage phenotype after ventilation

We further determined the expression level of Mac3 and CD206 in lung tissue after ventilation. As shown in Fig. 2A, on days 0 to 3, there were fewer CD206 and Mac3 positive cells in lung tissue, while on days 5, 7 and 14 after ventilation, there was a significant upregulation of the receptor CD206 and Mac3 in lungs than in sham. The results of flow cytometry showed the total number of cells isolated from the animals at each point in time after MV. It also indicated that, in both BALF cells or lung tissue cells, $CD45^+CD11b^+F4/80^+CD206^+$ cells were detectably activated on the 5th day and remained high for 2 weeks. By contrast, $CD45^+CD11b^+F4/80^+CD206^-$ macrophages mainly expressed these agents on days 0–3 (Fig. 2B–D). These data clearly indicate that high-VT MV induced a dramatically reprograming toward an upregulation of the CD206 and Mac3-positive cells and $CD45^+CD11b^+F4/80^+CD206^+$cells during the progression of fibrosis.

3.3. High-VT MV induced detectable EMT and activated TGF-β1/Smad2/3 signaling in VILI mice on day 7

EMT is an important pathological process related to ventilator-induced lung fibrosis. In our comparison among the sham and VILI groups on day 0 and day 7, we found a decreased expression level of epithelial marker of E-cadherin and increased expression levels of interstitial markers of vimentin and α-SMA in mice with high-VT MV on day 7 (Fig. 3A). Western blot results also indicated consistent E-cadherin loss and α-SMA and fibronectin initiation (Fig. 3B). Western blot analysis also suggested a higher levels of TGF-β1 and p-Smad2/3 expression in the VILI group on day 7 than in the sham and VILI groups on day 0 (Fig. 3C).

3.4. Primary M2 macrophages were closely associated with EMT and upregulated the TGF-β1/Smad2/3 signaling pathway in MLE-12 cells

In vitro experiments were performed to investigate the potential role of M2 macrophage polarization during the course of fibrosis. M0, M1, and M2 macrophages were isolated and identified in a standardized protocol (Fig. 4A, B). Fig. 4C indicated that the expression level of E-cadherin in MLE-12 cells was reduced, and the expression level of vimentin, α-SMA, and fibronectin were increased after co-culturing with M2 macrophages. Western blot analysis also indicated that a decreased level of E-cadherin and increased level of α-SMA (Fig. D). Additionally, the expression levels of TGF-β1 and p-Smad2/3 were both greater in MLE-12 cells co-cultured with M2 macrophages (Fig. E).

4. Discussion

In our prospective, randomized, controlled animal study, the data indicated that 1) high-VT MV could cause early inflammation and subsequent fibrosis in healthy mice without existing lung disease, which was consistent with findings we reported in a prior study; 2) high levels of VT MV induced a dramatically degree of M2 macrophage polarization during the progression of lung fibrosis. As shown, M2 macrophages were significantly increased at 5th day following ventilation and remained persistent high expression for 2 weeks. 3) high-VT MV caused lung EMT and up-regulation of TGF-β1, p-Smad2/3 at 7th

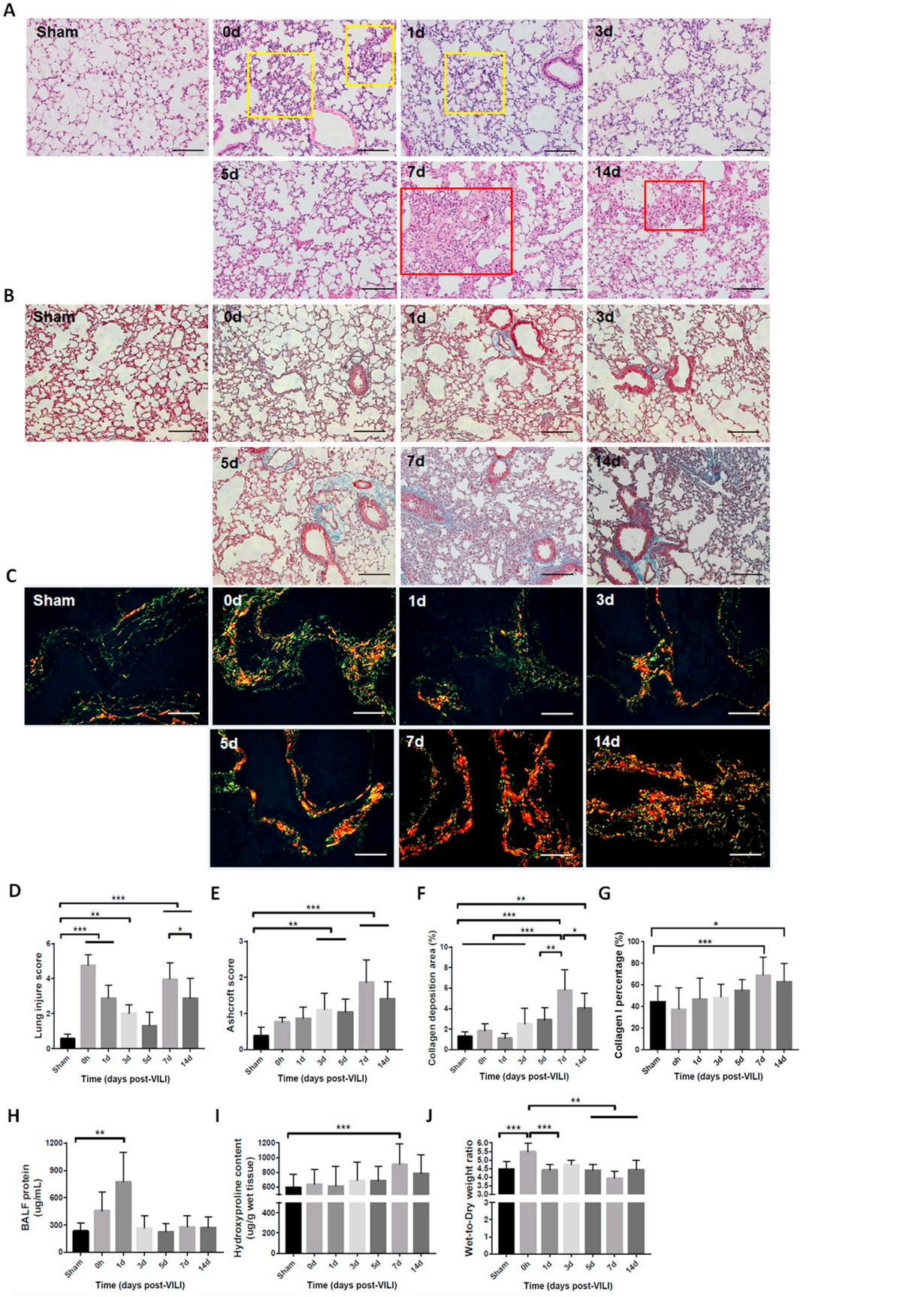

(caption on next page)

Fig. 1. Lung histopathology and fibrosis. (A) H&E staining. As shown in the yellow box in the images, the lung underwent alveolar hemorrhage and collapse with inflammatory cellular infiltration. The red box shows the aggravated alveolar collapse and thickened alveolar septum. These are suggestive of different phases of inflammation and fibrosis following ventilation. (B) Masson staining; green staining indicates collagen deposition. (C) Picrosirius Red staining; red and green colors indicate type I and III collagen, respectively. (Original images are × 20 magnification. n = 5–6; scale bar = 100 μm). (D) Lung injury score. (E) Lung fibrosis score. (F) The collagen deposition areas (%). (G) Collagen I percentage (%). Data were determined using the one-way ANOVA of 5–6 individuals. (H) The total protein in BALF. (I) Lung hydroxyproline content. (J) The wet-to-dry weight ratio. Data were determined using the one-way ANOVA of 8–10 individuals, and are presented as mean value ± SD. Significance is labeled as follows: $^{*}P < 0.05$, $^{**}P < 0.01$, $^{***}P < 0.001$. (For interpretation of the references to color in this figure legend, the reader is referred to the web version of this article.)

day after ventilation; 4) the co-culture of M2 macrophage and MLE-12 cells resulted in a significant EMT and activation of TGF-β1, p-Smad2/3 in MLE-12 cells. These observations support the concept that persistent tilt polarization toward M2 macrophages was associated with EMT during the course of ventilator-induced lung fibrosis, which may act by activating epithelial TGF-β1/Smad2/3 signaling.

Pulmonary macrophages are an essential part of lung innate immunity and host defense. They are characterized by heterogeneous and plasticity under local microenvironments. Existing data indicate can provide insight into macrophage phenotypes and functions. Briefly, macrophages are tethered to epithelial cells under homoeostatic states, with persistent expression of pattern recognition (TLRs) and scavenger (Dectin-1) receptors. Their turnover is slow, with minimal recruitment from circulating monocytes. Upon increased stimulation from foreign antigens, macrophage recruitment and activation takes place, skewing resident macrophages toward M1 macrophage, to help promote and sustain the inflammatory response. In pace with sufficient control of inflammation, macrophages start toward more reprograming of the M2 phenotype, which could play a featured role in inflammatory elimination and immunosuppression and promote tissue repair [6]. In some cases, the recruitment, resolution, and repair of macrophages are rapid (minutes to a few days) for minor cuts and tissue damage [8]. Even a more severe condition of myocardial injury can be repaired in a few days with the appropriate macrophages polarization and disappearance of M2 macrophages [20,21]. As shown, in our study, the macrophages in either BALF cell or lung tissue, demonstrated a remarkable increase in M1 macrophages during the inflammatory phase (days 0 to 3) and movement toward significant M2 activation state once the inflammation was controlled (days 3 to 5).

Notably, unlike from what had been proposed in normal repair, we witnessed a persistent M2 macrophage polarization, rather than any disappearance from the healing lungs. Although M2 polarization has been reported to play a role in the development of CODP and IPF, this study is the first to provide evidence of its relevance to ventilator-induced lung fibrosis. Here, we depicted a biological perspective that persistent M2 macrophage polarization can initiate and accelerate ventilator-induced lung fibrosis by some mechanism. For example, on day 5, lung histopathology showed a decline in pulmonary inflammatory response, and a slow repair in lung structure. By days 7 to 14, it developed into a significant fibrogenic lesion. Although this is not yet explained, we speculate that the lung microenvironment might play a role over time, and this role may be related to the different cells and their components during the different periods of the lung pathophysiology [34]. The role of macrophage phenotype differentiation should not be disregarded. We also found M2 macrophages to be more likely to be reprogramed in lung tissue than BALF cells were. We believe this might be related to the pathological injury of alveolar capillary membrane caused by high-VT ventilation. MV-induced inflammation rapidly depleted and damaged alveolar macrophages, requiring abundant replenishment of surviving macrophages from both interstitial macrophages and bone marrow to enter the alveolar space. Currently, some researchers have recognized that the current M1/M2 system is too simplistic to explain the refined macrophage phenotype spectrum, so a more refined system of classifying M2 macrophages has been described and found to be more accurate. These include M2a, M2b, M2c, and M2d subtypes [22,23].

In addition to macrophages, alveolar epithelial cells also participate in lung fibrogenesis. Studies showed inadequate alveolar epithelial repair and remodeling could act as an inciting factor for initiation and acceleration of ventilator-induced lung fibrosis [24]. Several mechanisms were considered. For example, the impaired capacity of proliferation and migration in alveolar epithelial cells and the inadequate differentiation of alveolar epithelial cells from their progenitor cells both contributed to the fibrosis [25]. Cabrera-Benítez. N E. et al. also suggested alveolar epithelial cells could serve as the progenitors for fibroblast-like cells via EMT [25]. Intriguingly, ETM has been increasingly recognized in the mediation of ventilator-induced lung fibrosis [27]. EMT refers to the transdifferentiation of epithelial cells into fibroblast-like cells, including morphologic transformation, phenotype marker transition, cytoskeletal rearrangements, and the activation of cell signaling pathways, which would eventually lead to fibrosis. In general, ZO-1, E-cad, SP-A, and SP-B are the most common epithelial markers; whereas vimentin, fibronectin, α-SMA, connective tissue growth factor (CTGF) and matrix metalloproteinases (MMPs) are the classic mesenchymal markers. During such biologic process that allows polarized epithelial cell transdifferentiation into mesenchymal cells a number of distinct growth factors triggered by inflammatory injury are engaged to initiate or complete an EMT, such as TGF-β, PDGF, and epidermal growth factor (EGF) [28]. Herein, TGF-β1 is considered the most important profibrotic cytokine. It triggers epithelial differentiation, collagen deposition, activation and proliferation of ECM-producing myofibroblasts [28]. Most importantly, our previous RNA sequencing revealed TGF-β1 pathways to be significantly enriched during fibrosis pathogenesis [10]. Because macrophages are one of the most prominent types of cells that accumulate at the site of injury and release TGF-β1, we hypothesized that the persistent activation of M2 macrophages may lead to EMT through activation of TGF-β1 signaling. Fortunately, in our vitro experiment, we did observe the co-localization of epithelial marker E-cadherin and the mesenchymal marker vimentin, the increased expression levels of mesenchymal marker, and the upregulation of TGF-β1/Smad2/3 signaling [19]. These data indicated that M2 macrophages play an important role in EMT and may play roles in the activation of epithelial TGF-β1/Smad2/3 signaling.

The parameters of VT and PEEP in mice differ considerably from the classical recommended parameters of ventilation seen in humans. During early 2000, the results of ARDSnet already suggested that, in ARDS patients, a low VT of 6–10 mL/kg with a relatively high PEEP would be necessary to prevent VILI in ARDS patients [31,32]. However, a well-defined and standard mouse model suitable for VILI or fibrosis would require a large VT of 20 mL/kg and 0 cm H_20 PEEP for several hours (typically 2–4 h) to cause inflammation in healthy lungs [11,33]. This is because lungs without pre-existing disease always need more mechanical stress to produce enough damage to create a useful model. In addition, the respiratory physiology of mice and humans also determines the differences in conditions between the two with respect to respiratory rate. Therefore, the values of these parameters seen in real-world "two-hit" human conditions are much smaller than those in the "one-hit" mouse model presented here, but for the purposes of this study, it is correct and feasible.

Other limitations are as follows: our data suggest that TGF/Smad2/3 signaling is activated during the course of fibrosis rather than via any specific mechanism involved in the fibrogenesis. Further research is

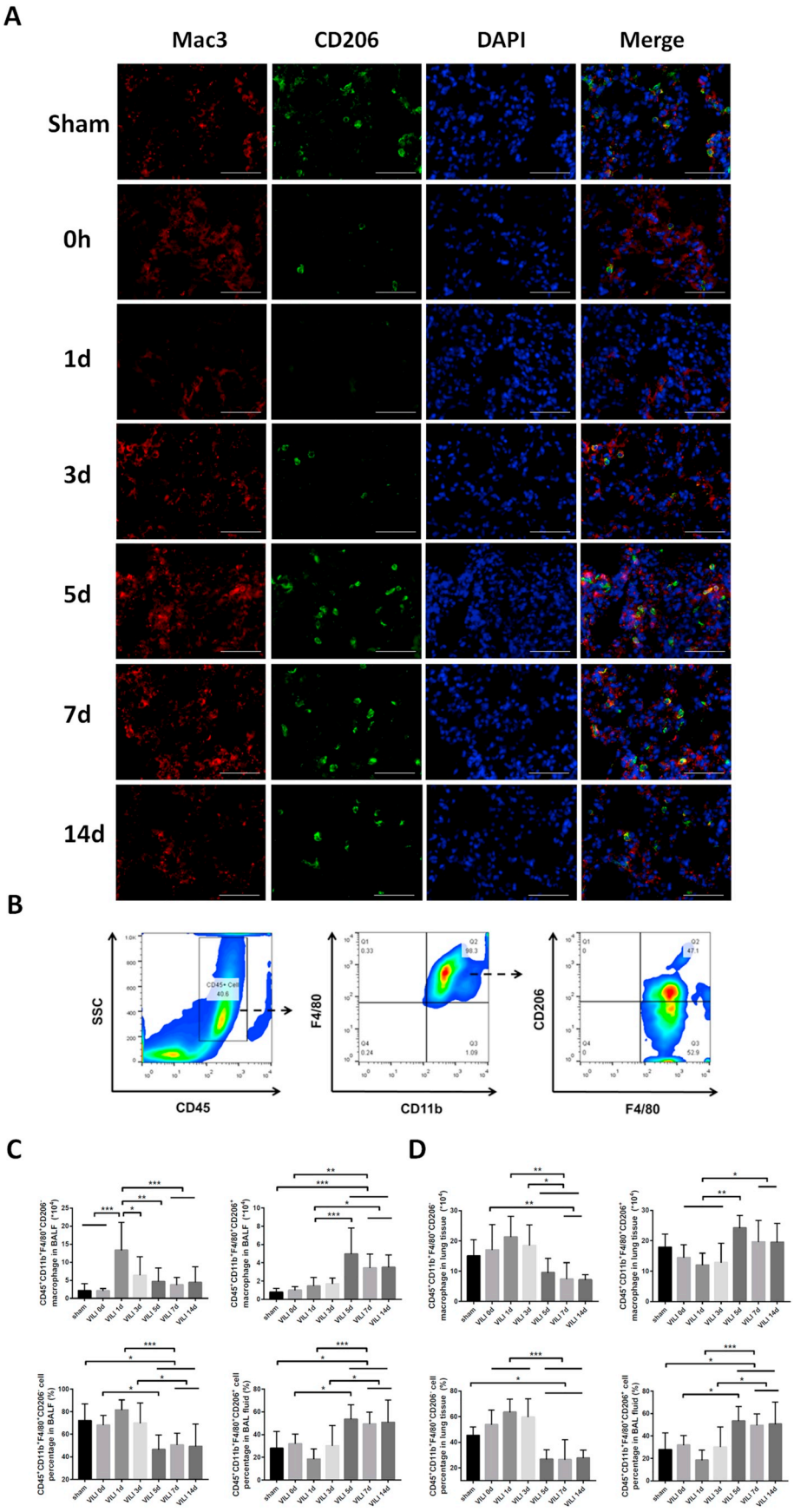

Fig. 2. Dynamic changes of macrophages polarization following ventilation.
(A) Double immunofluorescence stained for Mac3 and CD206. Red: Mac3; Green: CD206; Blue: DAPI. (Original images are × 400 magnification. n = 3–4; scale bar = 50 μm). (B) Representative flow cytometry gating to identify macrophage phenotype. Hematopoietic cells ($CD45^+$), pulmonary macrophages ($CD11b^+$, $F4/80^+$), M2 macrophages ($CD206^+$) were gated as shown. (C) Total number of cells isolated from the BALF and lung tissue. (D) Cell count and percentage of $CD45^+CD11b^+F4/80^+CD206^-$/$CD45^+CD11b^+F4/80^+CD206^+$ macrophage in BALF cell. (D) Cell count and percentage of $CD45^+CD11b^+F4/80^+CD206^-$/$CD45^+CD11b^+F4/80^+CD206^+$ macrophage in lung tissue. n = 8–12. Data were determined using the one-way ANOVA and were presented as mean value ± SD. Significance level is labeled as follows: $^*P < 0.05$, $^{**}P < 0.01$, $^{***}P < 0.001$. (For interpretation of the references to color in this figure legend, the reader is referred to the web version of this article.)

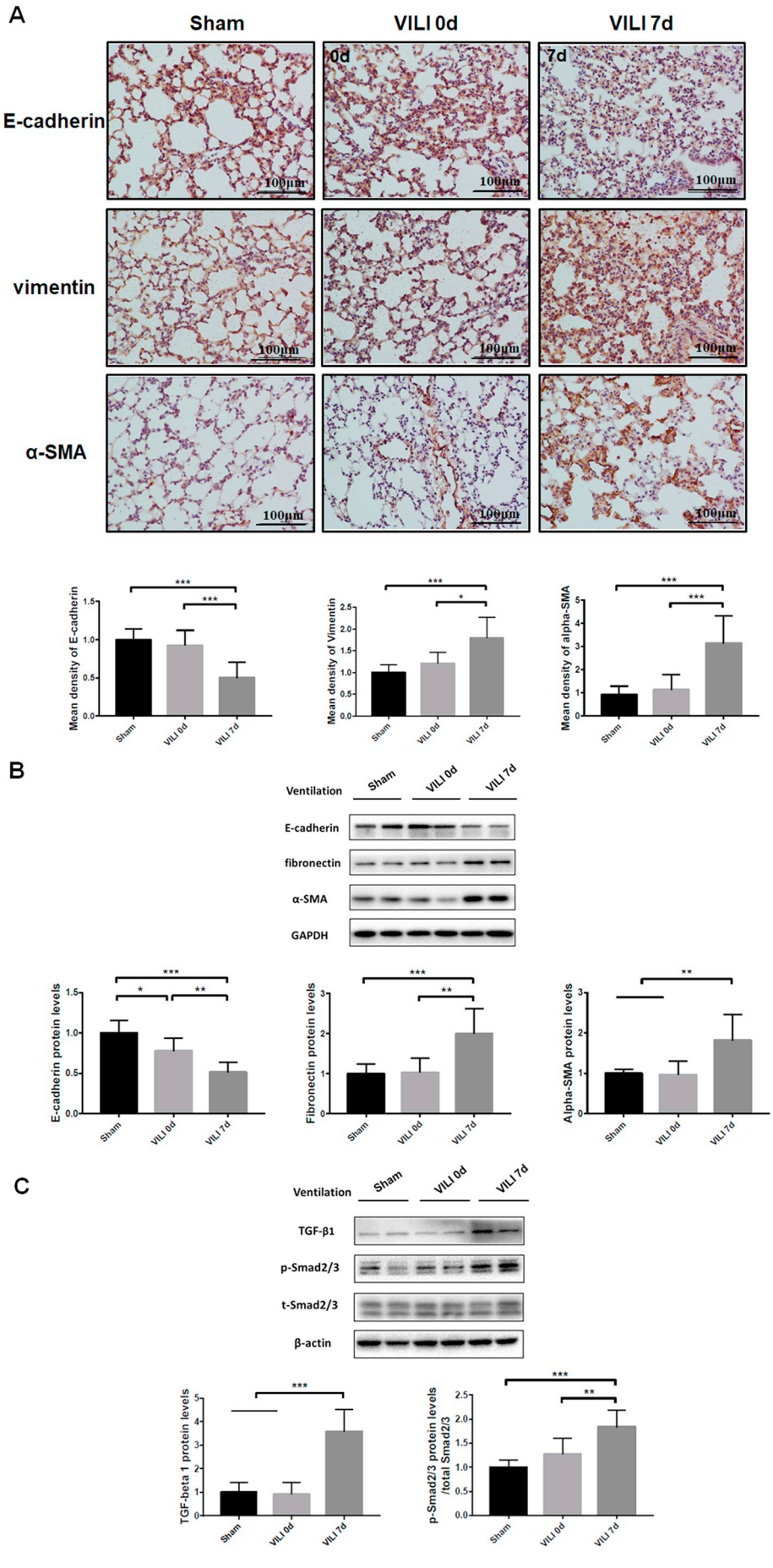

Fig. 3. EMT phenotype and TGF-β1/Smad2/3 signaling in lungs.(A) Immunohistochemical staining of E-cadherin, vimentin and α-SMA. Brown color indicates the positive areas. (Upper panel, original images are × 200 magnification. n = 5–6; scale bar = 100 μm). The mean density was expressed by fold-changes of ventilated lungs vs. Sham (lower panel). (B) Western blot analysis for each group. (C) Western blot analysis of TGF-β1, p-Smad2/3 in each group. All values were analyzed by using one-way ANOVA of 4 individuals, and were expressed by fold-changes of sham. Significance is labeled as follows: $^{*}P < 0.05$, $^{**}P < 0.01$, $^{***}P < 0.001$. (For interpretation of the references to color in this figure legend, the reader is referred to the web version of this article.)

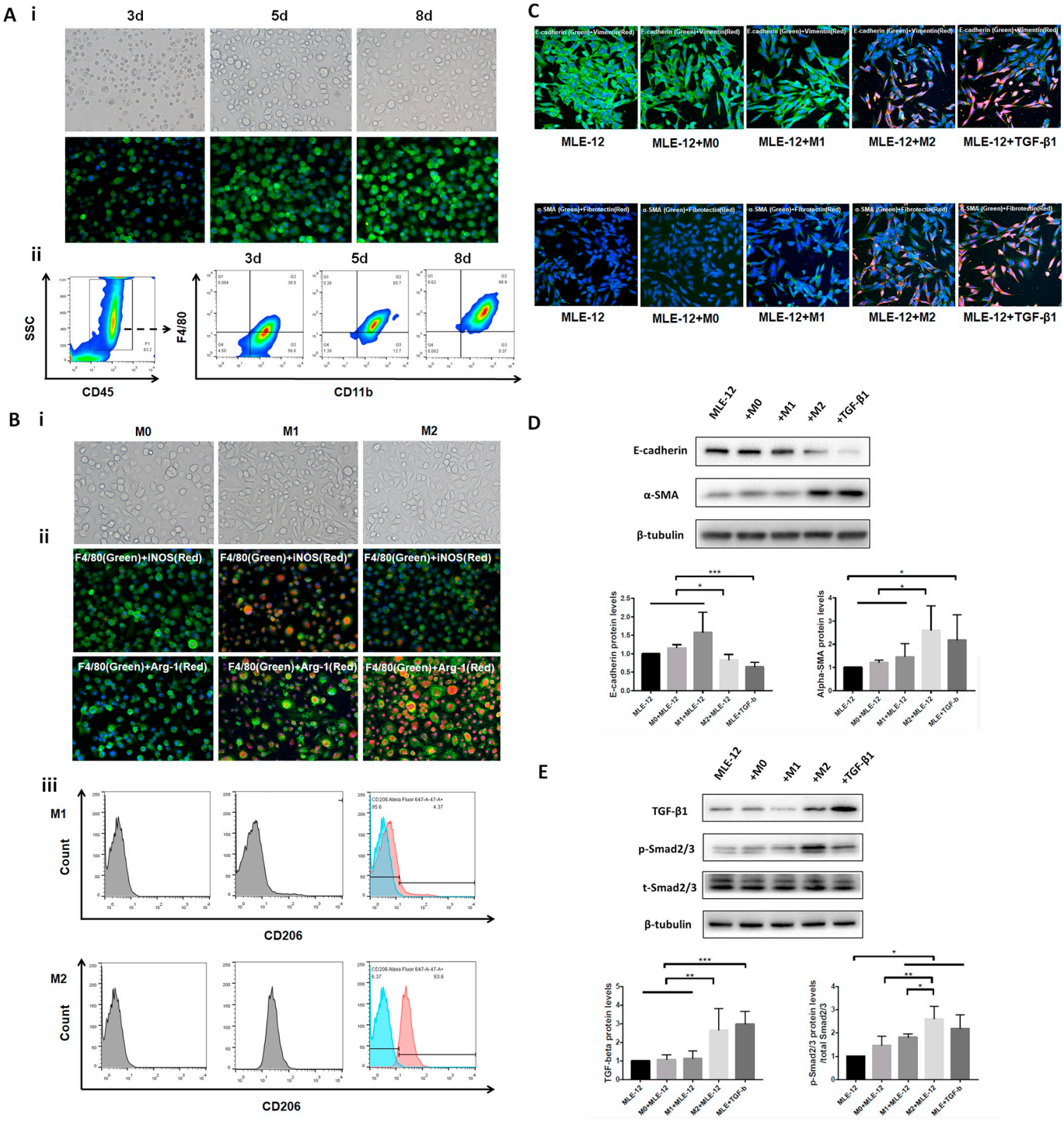

Fig. 4. EMT phenotype and TGF-β1/Smad2/3 signaling in MLE-12 cells.
(A) Identification of primary M0 macrophages: (i) Cell morphology and immunofluorescence of F4/80 on days 3, 5, and 8, respectively. (Original images are × 400 magnification; scale bar = 50 μm). (ii) Representative flow cytometry that gating to identify M0 macrophage. Hematopoietic cells ($CD45^+$), pulmonary macrophages ($CD11b^+$, $F4/80^+$). (B) Identification of M1/M2 macrophages. (i) Cell morphology. (ii) Dual-immunofluorescence staining for F4/80 and iNOS/Arg-1. (Original images are × 400 magnification; scale bar = 50 μm); (iii) Representative flow cytometry with gating to identify M1 and M2 macrophage. Hematopoietic cells ($CD45^+$), pulmonary macrophages ($CD11b^+$, $F4/80^+$), M2 macrophages ($CD206^+$) were gated as shown. (C) Dual-immunofluorescence for E-cadherin and vimentin, α-SMA and fibronectin. (Original images are × 400 magnification; scale bar = 50 μm). (D) Western blot for E-cadherin, and α-SMA. (E) Western blots for TGF-β1, Smad2/3 and p-Smad2/3. All data were presented as the mean value ± SD of three independent experiments. Significance is labeled as follows: $^*P < 0.05$, $^{**}P < 0.01$, $^{***}P < 0.001$. (For interpretation of the references to color in this figure legend, the reader is referred to the web version of this article.)

required to confirm our findings by using target gene deficient animals or selective inhibition of M2 macrophage or pathway. Second, our co-cultural system was established in MLE-12 cell lines and primary M2 macrophages induced with extrinsic supply of IL-4 and IL-13, which allowed a partial vivo microenvironment that in real state. Additionally, current works have suggested the need a more refined M2 macrophage classification system with a more accurate function. Although our present study may not be optimal, we think it provides a

novel insight into the mechanisms underlying this process and may be of use to future studies.

Declaration of Competing Interest

The authors declare no competing interests.

Acknowledgments

We would like to thank the support from the National Key Research and Development Program of China (2016YFC1304300), National Natural Science Foundation of China (Project No. 81470270; No. 8140080765) and Chinese Academy of Medical Science of Innovation Fund for Medical Sciences (2018-I2M-1-003). We thank LetPub (www.letpub.com) for its linguistic assistance during the preparation of this manuscript.

References

[1] F. Alessandri, F. Pugliese, V.M. Ranieri, Mechanical ventilation: we have come a long way but still have a long road ahead, Lancet Respir. Med. 5 (2017) 922–924.
[2] G.F. Curley, J.G. Laffey, H. Zhang, A.S. Slutsky, Biotrauma and ventilator-induced lung injury, Chest 150 (2016) 1109–1117.
[3] A.S. Slutsky, V.M. Ranieri, Ventilator-induced lung injury, N. Engl. J. Med. 369 (2013) 2126–2136.
[4] G.U. Meduri, M.A. Eltorky, Understanding ARDS-associated fibroproliferation, Intensive Care Med. 41 (2015) 517–520.
[5] N.E. Cabrera-Benitez, J.G. Laffey, M. Parotto, P.M. Spieth, J. Villar, H. Zhang, et al., Mechanical ventilation–associated lung fibrosis in acute respiratory distress syndrome, Anesthesiology 121 (2014) 189–198.
[6] N.R. Aggarwal, L.S. King, F.R. D'Alessio, Diverse macrophage populations mediate acute lung inflammation and resolution, Am. J. Physiol.-Lung C 306 (2014) L709–L725.
[7] T.A. Wynn, A. Chawla, J.W. Pollard, Macrophage biology in development, homeostasis and disease, Nature 496 (2013) 445–455.
[8] P.J. Murray, Macrophage polarization, Annu. Rev. Physiol. 79 (2017) 541–566.
[9] L. Zhang, Y. Wang, G. Wu, W. Xiong, W. Gu, C.Y. Wang, Macrophages: friend or foe in idiopathic pulmonary fibrosis? Respir. Res. 19 (2018) 170.
[10] L. Wang, N. Zhang, Y. Zhang, J. Xia, Q. Zhan, C. Wang, Landscape of transcription and long non-coding RNAs reveals new insights into the inflammatory and fibrotic response following ventilator-induced lung injury, Respir. Res. 19 (2018) 122.
[11] J. Villar, N.E. Cabrera, M. Casula, F. Valladares, C. Flores, J. López-Aguilar, et al., WNT/β-catenin signaling is modulated by mechanical ventilation in an experimental model of acute lung injury, Intensive Care Med. 37 (2011) 1201–1209.
[12] L.F. Li, P.H. Chu, C.Y. Hung, W.W. Kao, M.C. Lin, Y.Y. Liu, et al., Lumican regulates ventilation-induced epithelial-mesenchymal transition through extracellular signal-regulated kinase pathway, Chest 143 (2013) 1252–1260.
[13] J. Costello, B. Higgins, M. Contreras, M.N. Chonghaile, P. Hassett, D. O'Toole, et al., Hypercapnic acidosis attenuates shock and lung injury in early and prolonged systemic sepsis, Crit. Care Med. 37 (2009) 2412–2420.
[14] T. Ashcroft, J.M. Simpson, V. Timbrell, Simple method of estimating severity of pulmonary fibrosis on a numerical scale, J. Clin. Pathol. 41 (1988) 467–470.
[15] L. Zeng, S. Yang, C. Wu, L. Ye, Y. Lu, Effective transduction of primary mouse blood- and bone marrow-derived monocytes/macrophages by HIV-based defective lentiviral vectors, J. Virol. Methods 134 (2006) 66–73.
[16] B.K. Davis, Derivation of macrophages from mouse bone marrow, Methods Mol. Biol. 2019 (1960) 41–55.
[17] A.A. Tarique, J. Logan, E. Thomas, P.G. Holt, P.D. Sly, E. Fantino, Phenotypic, functional and plasticity features of classical and alternatively activated human macrophages, Am. J. Respir. Cell Mol. 53 (2015) 676.
[18] A. Sueki, K. Matsuda, C. Iwashita, C. Taira, N. Ishimine, S. Shigeto, et al., Epithelial-mesenchymal transition of A549 cells is enhanced by co-cultured with THP-1 macrophages under hypoxic conditions, Biochem. Biophys. Res. Commun. 453 (4) (2014) 804–809.
[19] L. Zhu, X. Fu, X. Chen, X. Han, P. Dong, M2 macrophages induce EMT through the TGF-β/smad2 signaling pathway, Cell Biol. Int. 41 (2017) 960–968.
[20] Y. Cheng, J. Rong, Macrophage polarization as a therapeutic target in myocardial infarction, Curr. Drug Targets 19 (2018) 651–662.
[21] V. Ryabov, A. Gombozhapova, Y. Rogovskaya, J. Kzhyshkowska, M. Rebenkova, R. Karpov, Cardiac CD68 + and stabilin-1 + macrophages in wound healing following myocardial infarction: from experiment to clinic, Immunobiology 223 (2018) 413–421.
[22] S. Colin, G. Chinetti-Gbaguidi, B. Staels, Macrophage phenotypes in atherosclerosis, Immunol. Rev. 262 (2014) 153–166.
[23] L. Reyes, T.G. Golos, Hofbauer cells: their role in healthy and complicated pregnancy, Front. Immunol. 9 (2018) 2628.
[24] T.A. Wynn, Integrating mechanisms of pulmonary fibrosis, J. Exp. Med. 208 (2011) 1339–1350.
[25] N.E. Cabrera-Benitez, M. Parotto, M. Post, B. Han, P.M. Spieth, W.E. Cheng, et al., Mechanical stress induces lung fibrosis by epithelial-mesenchymal transition, Crit. Care Med. 40 (2012) 510–517.
[27] L.F. Li, K.C. Kao, Y.Y. Liu, C.W. Lin, N.H. Chen, C.S. Lee, et al., Nintedanib reduces ventilation-augmented bleomycin-induced epithelial-mesenchymal transition and lung fibrosis through suppression of the Src pathway, J. Cell. Mol. Med. 21 (2017) 2937–2949.
[28] R. Kalluri, R.A. Weinberg, The basics of epithelial-mesenchymal transition, Clin. Invest. 119 (2009) 1420–1428.
[31] N. Ards, Ventilation with lower tidal volume as compared with traditional tidal volumes for acute lung injury. The acute respiratory distress syndrome network, New Engl. J. Med. 342 (2000) 1301–1308.
[32] D.G. De, T.M. Del, L. Rustichini, et al., ARDSNet lower tidal volume ventilatory strategy may generate intrinsic positive end-expiratory pressure in patients with acute respiratory distress syndrome, Am. J. Respir. Crit. Care 165 (2002) 1271–1274.
[33] M.R. Wilson, B.V. Patel, M. Takata, Ventilation with "clinically relevant" high tidal volumes does not promote stretch-induced injury in the lungs of healthy mice[J], Crit. Care Med. 40 (10) (2012) 2850–2857.
[34] D. Islam, Y. Huang, V. Fanelli, et al., Identification and modulation of microenvironment is crucial for effective MSC therapy in acute lung injury, Am J Respir Crit Care Med 199 (2019) 1214–1224.